

Effect of flux-dependent Friedel oscillations upon the effective transmission of an interacting nano-system

Axel Freyn and Jean-Louis Pichard

Service de Physique de l'Etat Condensé (CNRS URA 2464), DSM/DRECAM/SPEC,
CEA Saclay, 91191 Gif sur Yvette Cedex, France

November 1, 2018

Abstract. We consider a nano-system connected to measurement probes via non interacting leads. When the electrons interact inside the nano-system, the coefficient $|t_s(E_F)|^2$ describing its effective transmission at the Fermi energy E_F ceases to be local. This effect of electron-electron interactions upon $|t_s(E_F)|^2$ is studied using a one dimensional model of spinless fermions and the Hartree-Fock approximation. The non locality of $|t_s(E_F)|^2$ is due to the coupling between the Hartree and Fock corrections inside the nano-system and the scatterers outside the nano-system via long range Friedel oscillations. Using this phenomenon, one can vary $|t_s(E_F)|^2$ by an Aharonov-Bohm flux threading a ring which is attached to one lead at a distance L_c from the nano-system. For small distances L_c , the variation of the quantum conductance induced by this non local effect can exceed $0.1(e^2/h)$.

PACS. 71.27.+a Strongly correlated electron systems; heavy fermions – 72.10.-d Theory of electronic transport; scattering mechanisms – 73.23.-b Electronic transport in mesoscopic systems

1 Introduction

In the scattering approach [1, 2, 3] to quantum transport, the measure of the quantum conductance g of a nano-system requires incoherent electron reservoirs at a temperature T and metallic contacts (non interacting leads). For a two-probe measurement and one dimensional (1d) leads, g (in units of e^2/h for spin polarized electrons) is given in the limit $T \rightarrow 0$ by the probability $|t_s(E_F)|^2$ that an electron emitted from one reservoir at the Fermi energy E_F can be transmitted to the other reservoir through the nano-system and its attached leads. If the electron-electron interactions are negligible inside the nano-system, $|t_s(E_F)|^2$ is a local quantity which is independent of other scatterers that the attached leads can have. If the electrons interact inside the nano-system, the definition of $|t_s(E_F)|^2$ becomes much more subtle, since the nano-system is no longer a one body scatterer, but a many-body scatterer. Fortunately, a many body scatterer with two attached non interacting leads behaves when $T \rightarrow 0$ as an effective one body scatterer with interaction dependent parameters, and its effective one body transmission determines its quantum conductance.

A numerical proof of this statement is given in Ref. [4], based on the study of a ring made of a 1d auxiliary lead embedding a nano-system. The electrons were assumed without interaction unless being inside the nano-system. The persistent current I was numerically calculated as a function of the flux Φ piercing the ring. The values of $I(\Phi)$ were accurately determined using the DMRG algo-

rithm [5, 6] for an auxiliary lead of length L_L , and extrapolated to their limits as $L_L \rightarrow \infty$. The extrapolated values of $I(\Phi)$ calculated when an interaction of strength U acts inside the nano-system were shown to be identical to those given by a one body scatterer with an interaction dependent transmission coefficient $|t_s(E_F, U)|^2$. The embedding method [4, 7, 8, 9, 10, 11, 12, 13] consists in obtaining $|t_s(E_F, U)|^2$ from the extrapolated values of $I(\Phi)$.

However, an important difference between the many body problem and the one body problem is pointed out in Ref. [14]. Studying two identical interacting nano-systems in series by the embedding method, one finds that the value of $|t_s(E_F, U)|^2$ characterizing the transmission of the first nano-system is modified by the presence of the second nano-system. L_c being the length of the ideal wire coupling the two nano-systems, the correction induced by the second nano-system upon the effective transmission $|t_s(E_F, U)|^2$ of the first nano-system decays as $1/L_c$, with oscillations of period equal to half the Fermi wave length $\lambda_F/2$. This decay characterizes also the Friedel oscillations of the electron density induced by a scatterer inside a 1d non interacting electron gas. The presence of this correction to $|t_s(E_F, U)|^2$ shows us that this is not the interacting nano-system itself, but the nano-system with its contacts (attached leads and embedded scatterers) which is described by $|t_s(E_F, U)|^2$. The decay of this correction suggests that it is a consequence of the Friedel oscillations of the conduction electrons inside the coupling wire, which are caused by the two nano-systems in series.

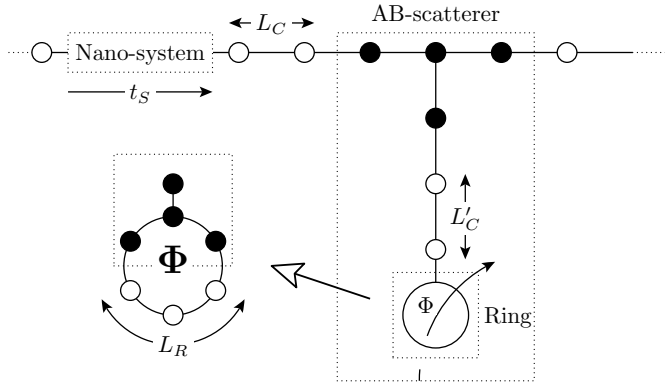


Fig. 1. Considered set-up made of a many body scatterer of effective transmission $|t_s|^2$ with two semi-infinite 1d leads: Polarized electrons interact only inside the nano-system (two sites with inter-site repulsion U , hopping term t_d and site potentials (gate voltage) V_G). A ring is attached at a distance L_c from the nano-system. The nano-system is described in more details in Fig. 4.

If the DMRG studies can give accurate results, the Hartree-Fock (HF) approximation has the merit to give a simple explanation for this non local transmission. This was done in Ref. [15], considering the Hartree and Fock corrections due to a local interaction inside a nano-system. In a tight-binding model, the Hartree corrections modify the site potentials seen by a transmitted electron, while the exchange terms give corrections to the hopping integrals. These HF corrections probe energy scales below E_F and length scales larger than the size of the nano-system inside which the electrons interact. Putting a second scatterer at a distance L_c from the interacting nano-system induces Friedel oscillations of the electron density inside the nano-system, which change the nano-system HF corrections. This means that the effective scattering properties of interacting nano-systems in series are coupled between themselves, exactly as are coupled magnetic moments by the RKKY interactions [16, 17, 18, 19].

This effect was studied in a previous letter [20], assuming a set-up which can be convenient for an experimental check of the theory: an infinite 1d tight-binding model of spin polarized electrons (spinless fermions), embedding two scatterers separated by L_c sites, as sketched in Fig. 1. The first scatterer is the nano-system inside which the electrons interact, while the second contains an attached ring. Hereafter, we refer to the second scatterer with its attached ring as the AB-scatterer, since an Aharonov-Bohm (AB) flux Φ can pierce the ring, its variations inducing periodic AB-oscillations of the electron density inside the nano-system. This yields flux dependent HF corrections for the nano-system, and hence AB-oscillations of its effective transmission $|t_s|^2$. This non local effect upon $|t_s|^2$ induced by a ring attached at L_c sites from the nano-system is a pure many body effect which was the subject of Ref. [20]. In this longer paper, a detailed derivation of the results summarized in Ref. [20] is given, with new analytical and numerical results showing how one can make this effect very large.

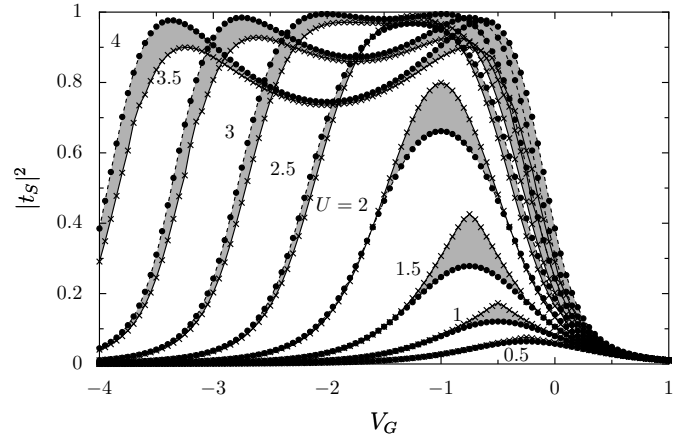


Fig. 2. Effective transmission $|t_s|^2$ as a function of the gate voltage V_G , at half filling (Fermi momentum $k_F = \pi/2$) and for a nano-system hopping term $t_d = 0.1$. The AB-scatterer with its attached ring ($L'_c = 4, L_R = 7$) is at $L_c = 2$ sites from the nano-system. The interaction strength U is indicated in the figure. A flux $\Phi = 0$ (\bullet) or $\Phi = \Phi_0/2$ (\times) threads the ring. The grey areas underline the effect of Φ upon $|t_s|^2$.

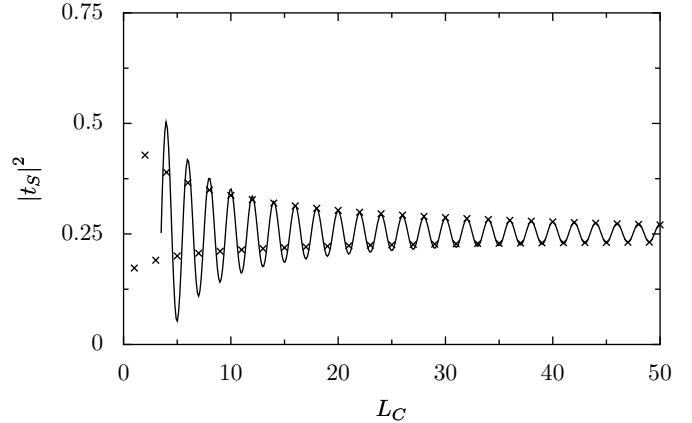


Fig. 3. $|t_s|^2$ as a function of the length L_c between the nano-system and the ring when $\Phi = 0$: The effect of the ring upon $|t_s|^2$ (see Fig. 2) decays as Friedel oscillations. HF results (\times) and fit $0.2522 + \cos(\pi L_c)/L_c$ (solid line), calculated for $V_G = -0.75$ and $U = 1.5$ ($L'_c = 4, L_R = 7, k_F = \pi/2, t_d = 0.1$).

Using the set-up sketched in Fig. 1, the non local effect upon $|t_s|^2$ is illustrated in Fig. 2. The nano-system effective transmission $|t_s|^2$ is given as a function of a gate voltage V_G applied upon the nano-system, at half filling (Fermi momentum $k_F = \pi/2$). For each strength U of a nearest neighbor repulsion acting inside the nano-system, two curves give $|t_s|^2$ as a function of V_G when the ring is attached near the nano-system ($L_c = 2$). The first curve (full circle) has been calculated when there is no flux Φ threading the ring, while the second one (cross) gives $|t_s|^2$ when half a flux quantum $\Phi_0/2$ threads the ring. If $U = 0$, the two curves are identical. The effect of U consists in changing the shape of the curves $|t_s(V_G)|^2$, and in making a difference underlined by grey areas between the cases where $\Phi = 0$ and $\Phi = \Phi_0/2$. Around certain values of V_G , the effect of Φ upon $|t_s|^2$ is of order 0.2 for a transmission

$|t_s|^2 \leq 1$. This means that one can make the effect huge if L_c is small, for well chosen values of the nano-system parameters. Fig. 3 shows how the effect of the ring upon $|t_s|^2$ decays as L_c increases. One can see the $\cos(2k_F L_c)/L_c$ asymptotic decay with even-odd oscillations characteristic of Friedel oscillations at half-filling.

In this paper, we explain the origin of the non local effects upon $|t_s|^2$ shown in Fig. 2. The paper is divided as follows. In section 2, the nano-system Hamiltonian is defined and the HF equations are given when it is embedded between two semi-infinite ideal leads. One gets two coupled equations which have to be solved self-consistently. The two equations are explicitly derived when the nano-system is not in series with another scatterer. A numerical method for having the HF parameters is then defined, which allows us to recover the results of the analytical derivations and to estimate its convergence when the size of the leads increases. In section 3, a simple limit where the HF parameters take trivial values is studied. In this limit, one can easily calculate the transmission $|t_s|^2$ as a function of V_G at a given strength U of the interaction, and explain the shape of the curves $|t_s(V_G)|^2$ shown in Fig. 2. Unfortunately, this limit is also the limit where the non local effect upon $|t_s|^2$ is negligible. For having large effects, one needs to be in the opposite limit. In section 4, the scatterer with the attached ring (AB-scatterer) is defined. Its scattering properties are calculated for each energy $E \leq E_F$. In section 5, the oscillations induced by the nano-system and by the AB-scatterer in the leads are studied separately, illustrating the phenomena responsible for the non locality of $|t_s|^2$. In section 6, one considers the interacting nano-system in series with the AB-scatterer, and we study the role of the gate potential V_G , the Fermi momentum k_F and the hopping term t_d upon the flux dependence of $|t_s|^2$. In section 7, the implications of the non locality of $|t_s|^2$ upon the total quantum conductance g_T are studied, when the nano-system is in series with the AB-scatterer between two measurement probes. We give a short summary in section 8, underlining the possible relevance of the many body effect described in this work for the theory of experiments imaging coherent electron flow from a quantum point contact in a two dimensional electron gas.

2 Hartree-Fock description of an interacting nano-system with non interacting leads

We consider a one dimensional tight-binding model of spin polarized electrons (spinless fermions), where the particles do not interact, unless they occupy two nearest neighbor sites (0 and 1), which costs an interaction energy U . The two sites 0 and 1, with potentials $V_0 = V_1 = V_G$, a repulsion U and an hopping term t_d define the nano-system. We assume that the potential V_G can be varied by a gate. The nano-system Hamiltonian reads

$$H_s = -t_d(c_0^\dagger c_1 + h.c.) + V_G(n_1 + n_0) + U n_1 n_0. \quad (1)$$

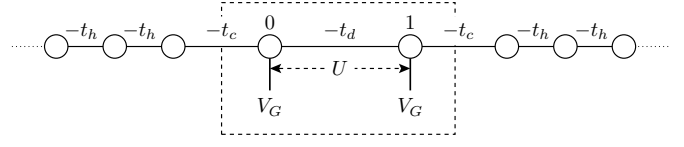


Fig. 4. Nano-system with two semi-infinite 1d leads: Spin polarized electrons interact only inside the nano-system (sites 0 and 1) with inter-site repulsion U and site-potentials $V_0 = V_1 = V_G$. The strength of the hopping terms is t_d inside the nano-system, t_c between the nano-system and the leads, and $t_h = 1$ in the leads.

c_p (c_p^\dagger) is the annihilation (creation) operator at site p , and $n_p = c_p^\dagger c_p$. The left (L) and right (R) leads are described by two Hamiltonians

$$H_{lead}^{L,R} = - \sum_p t_h (c_{p-1}^\dagger c_p + h.c.), \quad (2)$$

where p runs from $-\infty$ to -1 (3 to ∞) for the left (right) lead. The hopping amplitude in the leads $t_h = 1$ sets the energy scale, the conduction band corresponding to energies $-2 < E = -2 \cos k < 2$ (k real). The two leads and the nano-system are coupled by

$$H_{coupling}^{L,R} = -t_c (c_{p-1}^\dagger c_p + h.c.) \quad (3)$$

with $p = 2$ (0) for the coupling with the right (left) lead. The Hamiltonian

$$H = H_s + \sum_{J=L,R} (H_{lead}^J + H_{coupling}^J) \quad (4)$$

defines the interacting nano-system coupled with two non interacting 1d semi-infinite leads.

In the HF approximation, one takes for the ground state a Slater determinant of one-body wave-functions $\psi_\alpha(p)$ of energy $E_\alpha < E_F = -2 \cos k_F$. The $\psi_\alpha(p)$ are the eigenfunctions of the Hamiltonian H (Eq. 4), where the nano-system is described by an effective one body Hamiltonian

$$H_s^{HF} = -v(c_0^\dagger c_1 + h.c.) + V(n_1 + n_0) \quad (5)$$

instead of H_s . H_s^{HF} does not contain the two body term $U n_1 n_0$ of H_s (Eq. 1), but a renormalized hopping term v (instead of t_d), and a renormalized gate potential V (instead of V_G). The form of H_s^{HF} results from the nearest neighbor repulsion acting only between the sites 0 and 1, such that the exchange correction modifies only the strength of the hopping term t_d coupling those two sites, while the site-potentials V_0 and V_1 have two identical Hartree corrections, because of the reflection symmetry $p - 1/2 \rightarrow -p + 1/2$.

For the HF calculations, we proceed in three steps. All wave-functions $\psi_\alpha(p)$ of energy $E_\alpha \leq E_F$ are calculated for arbitrary values of v and V . Then, the expectation values

$$\begin{aligned} \langle c_0^\dagger c_1(v, V) \rangle &= \sum_{E_\alpha < E_F} \psi_\alpha^*(0) \psi_\alpha(1) \\ \langle c_0^\dagger c_0(v, V) \rangle &= \sum_{E_\alpha < E_F} \psi_\alpha^*(0) \psi_\alpha(0) \end{aligned} \quad (6)$$

are evaluated, either analytically or numerically. Eventually, the values of the two HF parameters v and V are adjusted till they converge towards the two self-consistent values which satisfy the coupled integral equations:

$$\begin{aligned} v &= t_d + U \langle c_0^\dagger c_1(v, V) \rangle \\ V &= V_G + U \langle c_0^\dagger c_0(v, V) \rangle \end{aligned} \quad (7)$$

Once the self-consistent values of v and V are numerically obtained from Eqs. (7), the effective transmission amplitude t_s of the nano-system at an energy $E_F = -2 \cos k_F$ reads:

$$t_s(U) = \frac{v(1 - e^{-2ik_F})}{v^2 - e^{-2ik_F} - 2Ve^{-ik_F} - V^2}. \quad (8)$$

2.1 Analytical form of the HF-equations

For the nano-system with two semi-infinite leads, the two first steps can be done analytically, while the last step requires to numerically solve the two coupled integral Eqs. (7). Let us derive the explicit expression of Eqs. (7). For simplicity, let us take $t_h = t_c = 1$.

The states $\psi_\alpha(p)$ are scattering states of energies $E_\alpha = -2 \cos k_\alpha$, which are inside the conduction band ($-2 \leq E_\alpha \leq 2$) of the leads, and bound states below ($E_\alpha < -2$) or above ($E_\alpha > 2$) this band. The contribution of the bound states to $\langle c_0^\dagger c_1 \rangle$ and $\langle c_0^\dagger c_0 \rangle$ is important, since they are centered inside the nano-system and decay exponentially outside.

The wave functions of the conduction band can be written in the leads as

$$\begin{aligned} \psi_{\alpha,+}(p) &= \frac{1}{\sqrt{2\pi}} \begin{cases} e^{ik_\alpha(p-\frac{1}{2})} + r_\alpha e^{-ik_\alpha(p-\frac{1}{2})} & \text{if } p \leq 0 \\ t_\alpha e^{ik_\alpha(p-\frac{1}{2})} & \text{if } p \geq 1 \end{cases} \\ \psi_{\alpha,-}(p) &= \frac{1}{\sqrt{2\pi}} \begin{cases} e^{-ik_\alpha(p-\frac{1}{2})} + r_\alpha e^{ik_\alpha(p-\frac{1}{2})} & \text{if } p \geq 1 \\ t_\alpha e^{-ik_\alpha(p-\frac{1}{2})} & \text{if } p \leq 0 \end{cases} \end{aligned} \quad (9)$$

where

$$\begin{aligned} r_\alpha &= \frac{e^{ik_\alpha}(-1 + v^2 - V^2 - 2V \cos k_\alpha)}{1 + 2Ve^{ik_\alpha} + (V^2 - v^2)e^{2ik_\alpha}} \\ t_\alpha &= \frac{v(e^{2ik_\alpha} - 1)}{-1 - 2Ve^{ik_\alpha} + (v^2 - V^2)e^{2ik_\alpha}}. \end{aligned} \quad (10)$$

There are 4 possible bound states centered on the nano-system. Their wave functions take the general form:

$$\psi_{bs}^{\alpha,\beta}(p) = A_{\alpha,\beta}(-1)^{p\alpha} \text{sign}(p\beta - \frac{\beta}{2}) e^{-K_{\alpha,\beta}|p-\frac{1}{2}|}. \quad (11)$$

Only two bound states of energies $E_{\alpha,\beta} = -2 \cosh(K_{\alpha,\beta})$ can exist below the conduction band. The first ($\alpha, \beta = 0, 1$) exists if $-(v+V) > 1$ with $K_{0,1} = \ln(-(v+V))$. The second ($\alpha, \beta = 0, 0$) exists if $v-V > 1$ with $K_{0,0} = \ln(v-V)$.

From Eqs. (9) and (11) the expectation values of $\langle c_0^\dagger c_1 \rangle$ and $\langle c_0^\dagger c_0 \rangle$ can be explicitly calculated. The contributions of the conduction band read

$$\begin{aligned} \langle c_0^\dagger c_1 \rangle_{cb} &= \sum_{q=\pm} \int_0^{k_F} \psi_{\alpha,q}(0)^* \psi_{\alpha,q}(1) dk_\alpha \\ &= \frac{F_- + 2v(k_F V + \Delta \sin k_F)}{2\pi \Delta^2} \\ \langle c_0^\dagger c_0 \rangle_{cb} &= \sum_{q=\pm} \int_0^{k_F} |\psi_{\alpha,q}(0)|^2 dk_\alpha \\ &= \frac{F_+ + k_F(v^2 + V^2 + \Delta^2) + 2V \Delta \sin k_F}{2\pi \Delta^2} \end{aligned} \quad (12)$$

respectively, where we have introduced different auxiliary functions:

$$\begin{aligned} \Delta &= v^2 - V^2 \\ f_0(\pm) &= \arctan \left(\frac{v \pm (V-1)}{v \pm (V+1)} \tan \frac{k_F}{2} \right), \\ f_\pm &= f_0(\pm) (\Delta^2 - (v \mp V)^2), \\ F_\pm &= f_+ \pm f_-. \end{aligned} \quad (13)$$

The contribution of the bound states reads:

$$\begin{aligned} \langle c_0^\dagger c_1 \rangle_{bs} &= \left(\frac{1}{2} - \frac{1}{2(v-V)^2} \right) \Theta(v-V-1) \\ &\quad + \left(-\frac{1}{2} + \frac{1}{2(v+V)^2} \right) \Theta(-v-V-1) \\ \langle c_0^\dagger c_0 \rangle_{bs} &= \left(\frac{1}{2} - \frac{1}{2(v-V)^2} \right) \Theta(v-V-1) \\ &\quad + \left(\frac{1}{2} - \frac{1}{2(v+V)^2} \right) \Theta(-v-V-1), \end{aligned} \quad (14)$$

where $\Theta(x)$ is the Heaviside step-function.

Using Eqs. (12) and (14) and

$$\begin{aligned} \langle c_0^\dagger c_1 \rangle &= \langle c_0^\dagger c_1 \rangle_{cb} + \langle c_0^\dagger c_1 \rangle_{bs} \\ \langle c_0^\dagger c_0 \rangle &= \langle c_0^\dagger c_0 \rangle_{cb} + \langle c_0^\dagger c_0 \rangle_{bs}, \end{aligned} \quad (15)$$

one gets an explicit form of the two integral Eqs. (7), which can be numerically solved for obtaining the self-consistent values of v and V .

2.2 Numerical method for having the HF parameters

If one includes other scatterers in the leads, to calculate the analytical form of the HF equations becomes tedious. It is faster to obtain v and V by an alternative numerical method, based on the numerical diagonalization of a one body system of size N , composed of H_S^{HF} coupled to two finite leads of size N_L and N_R , with $N_L \approx N_R$ and $N_R + N_L + 2 = N$. There are 4 possible cases: $N_L = N_R$ or $N_L = N_R + 1$ for N_L even or odd. Taking consecutive sizes $N, N+1, N+2$ and $N+3$, this gives the 4 different

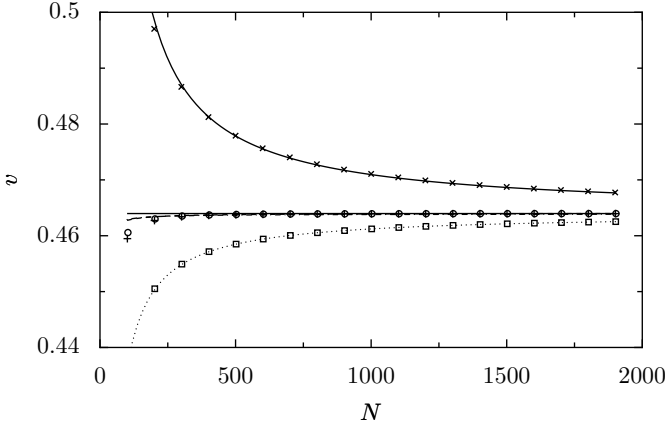


Fig. 5. Effective hopping term v of a nano-system with two finite 1d leads of respective lengths N_L and N_R ($N_L \approx N_R$) as a function of the total length $N = N_L + N_R + 2$, for $k_F = \pi/2$, $U = 2$, $t_h = t_c = 1$ and $t_d = 0.1$.

curves shown in Fig. 5, which converge towards the same asymptotic value v . This asymptotic value corresponds to the value obtained from the two coupled integral Eqs. (7) with the explicit form given by Eqs. (15).

3 Two limits for the Hartree-Fock approximation

3.1 Tractable limit ($t_d > t_h$, $|t_s|^2$ independent of external scatterers)

In the limit where t_d is large, such that $V_G - t_d \ll E_F$ and $V_G + t_d + U \gg E_F$, there is a large interval of values of V_G and E_F where the HF parameters read

$$\begin{aligned} v &= t_d + \frac{U}{2} \\ V &= V_G + \frac{U}{2}. \end{aligned} \quad (16)$$

For showing this, let us consider the case without interaction ($U = 0$). The one body Hamiltonian $H_0 = H_s(U = 0) + \sum_{J=L,R} (H_{lead}^J + H_{coupling}^J)$ gives rise to a $N \times N$ Hamiltonian matrix

$$\mathcal{H}_0 = \begin{pmatrix} \mathcal{H}_{lead}^L & \mathcal{H}_L & 0 \\ \mathcal{H}_L^\dagger & \mathcal{H}_A & \mathcal{H}_R \\ 0 & \mathcal{H}_R^\dagger & \mathcal{H}_{lead}^R \end{pmatrix} \quad (17)$$

in the site basis, where the 4×4 matrix

$$\mathcal{H}_4 = \begin{pmatrix} 0 & -t_c & 0 & 0 \\ -t_c & V_G & -t_d & 0 \\ 0 & -t_d & V_G & -t_c \\ 0 & 0 & -t_c & 0 \end{pmatrix} \quad (18)$$

describes the nano-system with its coupling to the leads. Assuming that the two leads have an equal length $N_L = N_R = L$, \mathcal{H}_{lead}^L (\mathcal{H}_{lead}^R) are the $(L-1) \times (L-1)$ matrices

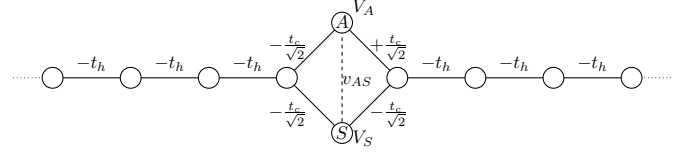


Fig. 6. Equivalent set-up obtained by the orthogonal transformation \mathcal{O} from the original set-up drawn in Fig. 4. The nano-system is now made of two sites in parallel connected to the 2 leads by modified hopping terms $\pm t_c/\sqrt{2}$. The site corresponding to the symmetric (anti-symmetric) orbital has an energy V_S (V_A) which is given by Eqs. (23). The hopping term v_{AS} due to exchange is zero when there is reflection symmetry.

describing the left (right) lead of size L (minus its last (first) site). \mathcal{H}_L (\mathcal{H}_R) are $(L-1) \times 4$ ($4 \times (L-1)$) matrices with a single non zero matrix element $-t_h$ describing the hopping between the lead and its last (first) site.

Let us introduce a $N \times N$ orthogonal transformation \mathcal{O} which contains a 4×4 matrix

$$\mathcal{O}_4 = \begin{pmatrix} 1 & 0 & 0 & 0 \\ 0 & \frac{1}{\sqrt{2}} & \frac{1}{\sqrt{2}} & 0 \\ 0 & \frac{1}{\sqrt{2}} & -\frac{1}{\sqrt{2}} & 0 \\ 0 & 0 & 0 & 1 \end{pmatrix} \quad (19)$$

acting upon \mathcal{H}_4 , such that

$$\mathcal{O}_4^T \mathcal{H}_4 \mathcal{O}_4 = \begin{pmatrix} 0 & -\frac{t_c}{\sqrt{2}} & -\frac{t_c}{\sqrt{2}} & 0 \\ -\frac{t_c}{\sqrt{2}} & V_S^0 & 0 & -\frac{t_c}{\sqrt{2}} \\ -\frac{t_c}{\sqrt{2}} & 0 & V_A^0 & +\frac{t_c}{\sqrt{2}} \\ 0 & -\frac{t_c}{\sqrt{2}} & +\frac{t_c}{\sqrt{2}} & 0 \end{pmatrix}, \quad (20)$$

where $V_A^0 = V_G + t_d$ and $V_S^0 = V_G - t_d$. \mathcal{O} leaves \mathcal{H} unchanged otherwise. Let us introduce the operators $d_S = (c_0 + c_1)/\sqrt{2}$ and $d_A = (c_0 - c_1)/\sqrt{2}$, corresponding respectively to the symmetric (antisymmetric) combination of the nano-system orbitals. $n_S = d_S^\dagger d_S$ and $n_A = d_A^\dagger d_A$. Since $n_1 n_0 = n_A n_S$, the HF equations (7) become in the transformed basis

$$\begin{aligned} V_A &= V_A^0 + U \langle d_S^\dagger d_S \rangle \\ V_S &= V_S^0 + U \langle d_A^\dagger d_A \rangle \\ v_{AS} &= U \langle d_A^\dagger d_S \rangle, \end{aligned} \quad (21)$$

where $v_{AS} = 0$, since

$$\langle d_A^\dagger d_S \rangle = \frac{1}{2} (\langle n_0 \rangle - \langle n_1 \rangle + \langle c_0^\dagger c_1 \rangle - \langle c_1^\dagger c_0 \rangle), \quad (22)$$

is equal to zero if the system is invariant under the inversion $0 \leftrightarrow 1$.

The equivalent set-up obtained by the orthogonal transformation \mathcal{O} from the original set-up is sketched in Fig. 6. There are three simple limiting cases: two correspond to the limit where either $V_A, V_S \ll E_F$ or $V_A, V_S \gg E_F$, such that the two sites of the nano-system are either totally filled or totally empty. This yields an effective

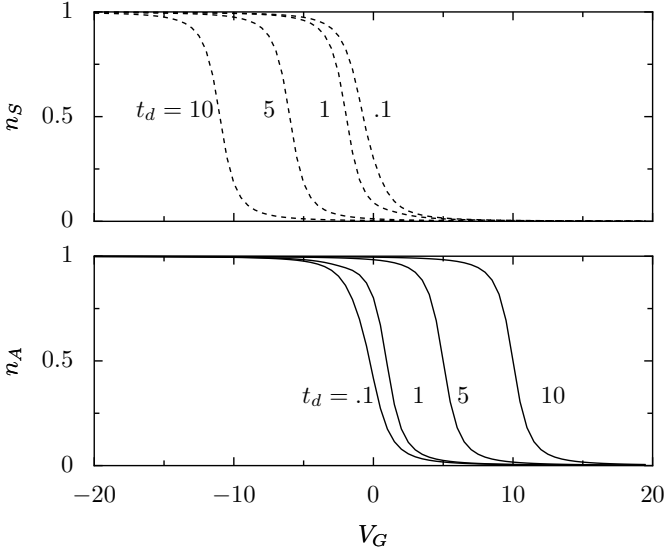


Fig. 7. Occupation numbers $\langle n_S \rangle$ (solid lines) and $\langle n_A \rangle$ (dashed lines) as a function of V_G for $k_F = \pi/8$ and different values of t_d given in the figure. $U = 1$, $t_c = t_h = 1$.

transmission $|t_s|^2 \approx 0$ at E_F . The third case corresponds to a site A (anti-symmetric orbital) with an occupation number $\langle n_A \rangle \approx 0$ ($V_A \gg E_F$) and a site S (symmetric orbital) with $\langle n_S \rangle \approx 1$ ($V_S \ll E_F$). The larger is t_d , the larger is the range of values of V_G corresponding to this limit, for a given Fermi energy E_F . In that case, Eqs. (21) give

$$\begin{aligned} V_A &= V_G + t_d + U \\ V_S &= V_G - t_d. \end{aligned} \quad (23)$$

Putting in the 4×4 matrix given by Eq. (20) those HF values V_A and V_S instead of the bare values V_A^0 and V_S^0 defines \mathcal{H}_4^{HF} . Calculating $\mathcal{O}_4 \mathcal{H}_4^{HF} \mathcal{O}_4^T$, one finds for the HF parameters V and v the values given by Eqs. (16).

Using the analytical form of HF equations given in subsection 2.1, we have calculated the two occupation numbers $\langle n_S \rangle$ and $\langle n_A \rangle$ as a function of V_G for different values of $E_F = -2 \cos k_F$ and t_d . The results are shown assuming a nano-system well coupled to the leads ($t_c = t_h = 1$), for $k_F = \pi/8$ (Fig. 7) and for $k_F = \pi/2$ (Fig. 8). One can see that for $t_d \gg 1$, there are large intervals of values of V_G for which $\langle n_S \rangle \approx 1$ and $\langle n_A \rangle \approx 0$. In that case, v and V are given by Eqs. (16) and it is very easy to obtain the nano-system transmission $|t_s|^2$ at the Fermi energy E_F . For renormalized hopping term v and gate potential V , the effective transmission reads

$$|t_s|^2 \approx \frac{v}{x} \left(\frac{\Gamma^2}{(v-x)^2 + \Gamma^2} - \frac{\Gamma^2}{(v+x)^2 + \Gamma^2} \right), \quad (24)$$

where

$$\begin{aligned} \Gamma &= t_c^2 \sin k_F \\ x &= V - (t_c^2 - 2) \cos k_F. \end{aligned} \quad (25)$$

If v and V are given by Eqs. (16), one finds:

$$|t_s|^2 \approx \Delta \left(\frac{\Gamma^2}{(V_G - V_1)^2 - \Gamma^2} - \frac{\Gamma^2}{(V_G - V_2)^2 - \Gamma^2} \right), \quad (26)$$

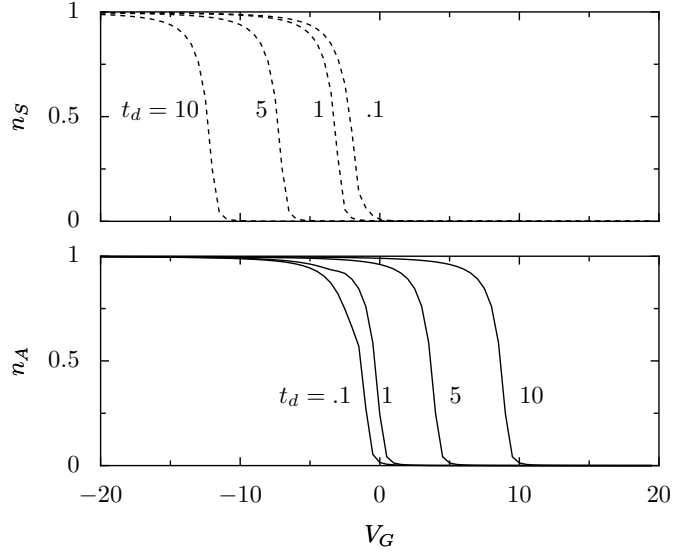


Fig. 8. Occupation numbers $\langle n_S \rangle$ (solid lines) and $\langle n_A \rangle$ (dashed lines) as a function of V_G for $k_F = \pi/2$ and different values of t_d given in the figure. $U = 1$, $t_c = t_h = 1$.

where

$$\begin{aligned} \Delta &= \frac{2t_d + U}{2V_G + U - 2(t_c^2 - 2) \cos k_F} \\ V_1 &= t_d + (t_c^2 - 2) \cos k_F \\ V_2 &= -t_d + (t_c^2 - 2) \cos k_F - U. \end{aligned} \quad (27)$$

When one varies V_G , Eq. (26) gives for the transmission $|t_s|^2$ two transmission peaks located at $V_G = V_1$ and V_2 , and spaced by a large interval $2t_d + U$ when t_d is large.

When $t_c \ll 1$, $(t_c^2 - 2) \cos k_F \approx E_F$ and the nano-system is very weakly coupled to the leads, with two levels of energy $V_G \pm t_d$ when $U = 0$. There are two sharp transmission peaks of width $\Gamma = t_c^2 \sin k_F \ll 1$, the first when $E_F \approx V_G - t_d$ ($V_G = V_1$), the second when $E_F \approx V_G + t_d + U$ ($V_G = V_2$). Since one needs an energy E_F for putting an electron outside the nano-system, and an energy $V_G - t_d$ to put an electron inside the empty nano-system, or $V_G + t_d + U$ inside the nano-system occupied by another electron, one recovers the usual Coulomb Blockade, where the nano-system has a transmission peak when it is indifferent for an electron to be inside or outside the nano-system.

When $t_c \rightarrow 1$, the nano-system becomes strongly coupled to the leads, the peak width Γ is broader and the two values of V_G for which the transmission is large are shifted by an amount equal to $E_F/2$.

This double peak structure is shown in Fig. 9 when $t_d \gg t_h$ and $t_c = t_h = 1$. It agrees with the curve given by Eq. (26). In contrast, this approximation totally fails to describe the single peak structure occurring when $t_d = 0.1$, as shown in Fig. 9 and Fig. 10.

When t_d is large, the symmetric site S of potential $V_S = V_G - t_d$ is far from the anti-symmetric site of potential $V_A = V_G + t_d + U$. If the nano-system is empty ($|t_s|^2 \approx 0$) and if one varies E_F for a given value of V_G , or V_G for a given value of E_F , one first fills the symmetric

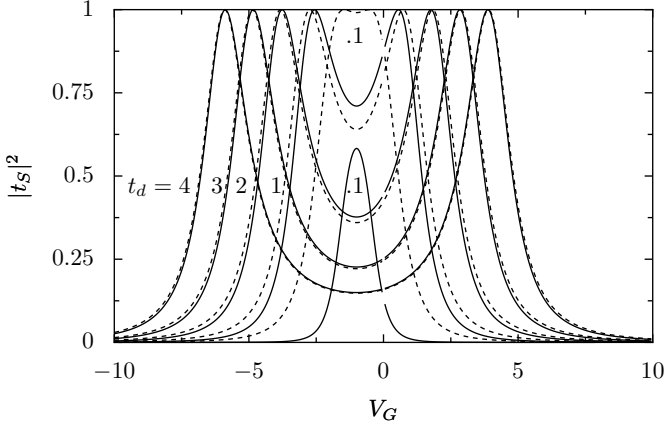


Fig. 9. Effective nano-system transmission $|t_s|^2$ as a function of V_G for $k_F = \pi/2$ and different values of t_d given in the figure. $U = 2$, $t_c = t_h = 1$. The solid lines give $|t_s|^2$ calculated using Eq. (24) with the HF parameters v and V calculated exactly. The dashed lines give $|t_s|^2$ calculated using Eq. (26) (v and V given by Eqs. (16)).

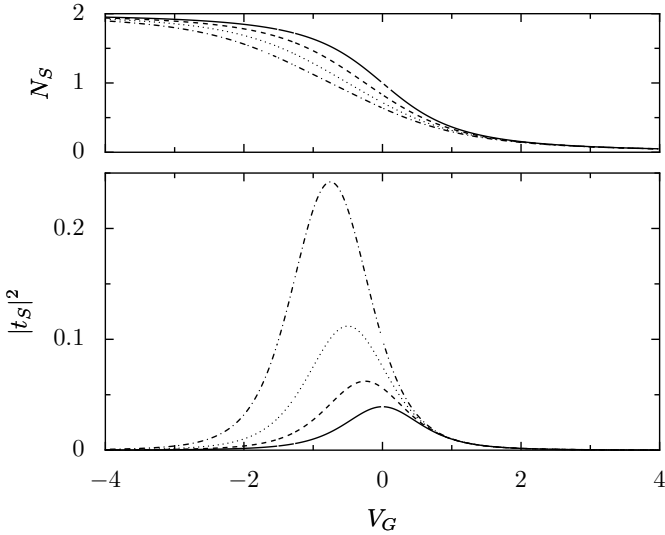


Fig. 10. $t_d = 0.1$, $k_F = \pi/2$, $t_c = t_h = 1$. Nano-system occupation number $N_S = \langle n_A \rangle + \langle n_S \rangle$ (up) and corresponding effective transmission $|t_s|^2$ (down) as a function of V_G for $U = 0$ (solid), 0.5 (dashed) 1 (dotted) 1.5 (dashed-dotted).

state, then the anti-symmetric one. This gives two transmission peaks. When the two potentials V_A and V_S are far from E_F , $\langle n_A \rangle$ and $\langle n_S \rangle$ are either 0 or 1, and only huge external Friedel oscillations could enter inside the nano-system and vary $|t_s|^2$. In that case, the nano-system occupation number $N_S = \langle n_A \rangle + \langle n_S \rangle$ is locked to values 0, 1 or 2, which cannot be changed by external Friedel oscillations. This makes the sensitivity of $|t_s|^2$ to external scatterers very negligible in that case. If one of the two renormalized potentials V_A and V_S is near E_F , only the component of external Friedel oscillations with the right symmetry can go through the equivalent site A or S of the same symmetry. Even in that case, the change of $|t_s|^2$ by an external scatterer cannot be very large. The limit

where the solution of HF equations is straightforward is also the limit where the nano-system transmission is almost independent of external scatterers.

3.2 Non local Limit ($t_d < t_h$, $|t_s|^2$ dependent of external scatterers)

When t_d is small, the symmetric site S of potential $V_G - t_d$ and the anti-symmetric site A of potential $V_G + t_d + U$ can be put together near E_F by a suitable strength of V_G . In that case, the two transmission peaks merge into a single one, as shown in Figs. 9 and 10 for $t_d = 0.1$. Looking in Figs. 7 and 8, one can see that $\langle n_A \rangle \approx \langle n_S \rangle$ take intermediate values between 0 and 1 around this single transmission peak, the potentials V_A and V_S being near E_F for the same values of V_G . This is the interesting limit where one can strongly vary $\langle n_A \rangle$ and $\langle n_S \rangle$ by external scatterers, the induced Friedel oscillations being able to enter inside the nano-system. Large variations of the HF parameters can be expected in this limit, and hence large changes of the effective transmission $|t_s|^2$. If the external scatterer is made of an attached ring, the induced Friedel oscillations entering inside the nano-system can be changed by an AB flux threading the ring, and $|t_s|^2$ can exhibit large AB oscillations.

4 Aharonov-Bohm scatterer

The AB-scatterer sketched in Fig. 1 contains an attached ring, such that it can induce flux dependent Friedel oscillations in the lead when an AB flux is varied through the ring. Its topology requires two 3-lead contacts (3LC). A 3LC is made of 4 coupled sites indicated by black circles in Fig. 1, and is described by a local Hamiltonian

$$H_P = \sum_{p=1}^3 -t_p (c_p^\dagger c_p + h.c.), \quad (28)$$

P denoting the central site and the sum p being taken over its 3 neighbors. The hopping terms are taken equal $t_p = t_h = 1$. The first 3LC allows us to attach a vertical lead to the horizontal lead, the second one to attach the ring to this vertical lead. L_c is the number of sites between the upper 3LC and the nano-system. Varying L_c , one can study the influence of the AB scatterer upon the effective transmission $|t_s|^2$ of the nano-system. L'_c and L_R are respectively the numbers of sites between the two 3LCs (length of the vertical lead) and of the attached ring (length of the ring without the three sites of the lower 3LC), as shown in Fig. 1. A 3×3 matrix $S_P(k)$ describes the scattering by a 3LC at an energy $E = -2 \cos k$:

$$S_P(k) = \begin{pmatrix} s_d & s_o & s_o \\ s_o & s_d & s_o \\ s_o & s_o & s_d \end{pmatrix} \quad (29)$$

where

$$\begin{aligned} s_d &= \frac{-e^{ik}}{3e^{ik} - 2\cos k} \\ s_o &= \frac{2i\sin k}{3e^{ik} - 2\cos k}. \end{aligned} \quad (30)$$

The reflection amplitude of an incoming electron of the vertical lead by the ring threaded by a flux Φ reads

$$r_R(\varphi) = \frac{h_k(\varphi) - \sin(kL_R)}{-h_k(\varphi) + e^{2ik}\sin(kL_R)}, \quad (31)$$

where

$$h_k(\varphi) = 2e^{ik}(\cos(kL_R) - \cos\varphi)\sin k \quad (32)$$

$\phi = 2\pi\Phi/\Phi_0$, Φ_0 being the flux quantum.

The reflection and transmission amplitudes of an electron moving in the horizontal lead by the AB-scatterer read

$$r_{AB}(k) = \frac{-e^{2ik} - e^{2ikL'_c}r_R(\varphi)}{2e^{2ik} - 1 + r_R(\varphi)e^{2ik(L'_c+1)}} \quad (33)$$

$$t_{AB}(k) = \frac{2i\sin ke^{ik}(1 + e^{2ikL'_c}r_R(\varphi))}{2e^{2ik} - 1 + r_R(\varphi)e^{2ik(L'_c+1)}}. \quad (34)$$

5 Friedel oscillations and particle-hole symmetry

If one puts a symmetric nano-system in series with an AB-scatterer, the inversion symmetry is broken, and the potentials $V_0 \neq V_1$. In that case, one has to calculate the values v , V_0 and V_1 of the HF parameters satisfying the three coupled HF equations

$$\begin{aligned} v &= t_d + U \langle c_0^\dagger c_1(v, V_0, V_1) \rangle \\ V_0 &= V_G + U \langle c_1^\dagger c_1(v, V_0, V_1) \rangle \\ V_1 &= V_G + U \langle c_0^\dagger c_0(v, V_0, V_1) \rangle, \end{aligned} \quad (35)$$

instead of the two HF Eqs. (7) valid when $V_0 = V_1$.

The non local effect is a consequence of the corrections to $\langle c_0^\dagger c_1 \rangle$, $\langle c_0^\dagger c_0 \rangle$ and $\langle c_1^\dagger c_1 \rangle$ which are induced inside the nano-system by the AB scatterer. In the general case, the AB scatterer and the nano-system induce at a site p Friedel oscillations of the density $\langle c_p^\dagger c_p \rangle$ and similar oscillations of the correlation function $\langle c_p^\dagger c_{p+1} \rangle$. Let us illustrate the effect of each scatterer inside the attached leads when there is particle-hole symmetry. In this particular case, the density stays uniform, $\langle c_p^\dagger c_p \rangle = 1/2$ everywhere and there are no Friedel oscillations of the density. But the effect of the AB scatterer upon the nano-system transmission $|t_s|^2$ persists, because of the exchange contribution, and one just needs to study $\langle c_p^\dagger c_{p+1} \rangle$. Particle-hole symmetry occurs at half-filling ($k_F = \pi/2$) when one takes a gate potential $V_G = -U/2$ which exactly compensates the Hartree contributions $U/2$, such that $V_0 = V_1 = 0$.

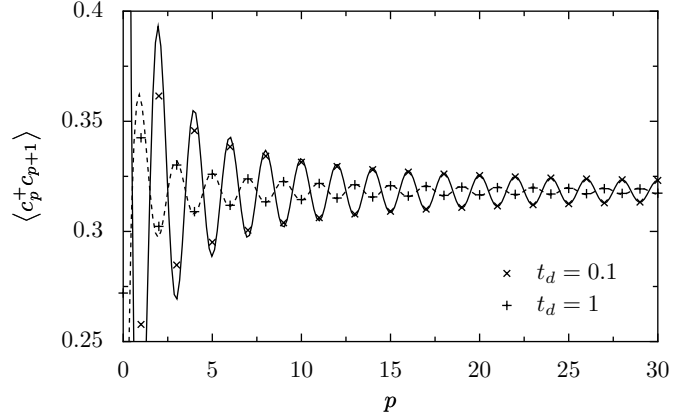


Fig. 11. Even-odd oscillations of $\langle c_p^\dagger c_{p+1} \rangle$ towards the asymptotic value $1/\pi$, induced inside the leads by the interacting nano-system for $k_F = \pi/2$, $U = 1$, $V_G = -U/2$ and $t_c = t = 1$. The dashed and solid lines give two asymptotic fits $1/\pi + b\cos(\pi p + c)/p$ with ($b = 0.04151$, $c = \pi$) and ($b = 0.14776$, $c = 0$) for $t_d = 1$ (+) and $t_d = 0.1$ (x) respectively.

5.1 Interaction dependent oscillations induced by the nano-system

In a case where particle-hole symmetry yields a uniform density, the usual Friedel oscillations are absent, and the exact form of $\langle c_p^\dagger c_{p+1} \rangle$ is given in Ref. [15] for $V_G = -U/2$ and $t_d = 1$. It has an asymptotic behavior which reads

$$\langle c_p^\dagger c_{p+1} \rangle \approx a + b \frac{\cos(2k_F p + c)}{p}, \quad (36)$$

where the asymptotic value $a = \sin k_F/\pi$ and the phase $c = 0$ at $k_F = \pi/2$. This gives even-odd oscillations with a $1/p$ -decay towards the asymptotic value $1/\pi$ which are shown in Fig. 11 for $t_d = 1$ and $t_d = 0.1$. As expected, the amplitude $b = 0.14776$ is larger when $t_d = 0.1$ than when $t_d = 1$ ($b = 0.04151$). The asymptotic form given by Eq. (36) characterizes also the Friedel oscillations of $\langle c_p^\dagger c_p \rangle$ when particle-hole symmetry is broken.

5.2 Flux dependent oscillations induced by the AB scatterer

The AB scatterer induces also flux dependent oscillations of $\langle c_p^\dagger c_{p+1} \rangle$ around it, even though $\langle c_p^\dagger c_p \rangle = 1/2$ everywhere if $k_F = \pi/2$. These oscillations have also the asymptotic behavior given by Eq. (36), as shown in Fig. 12 and 13 for even and odd sizes L_R of the ring ($L_R = 6$ and 7). At $k_F = \pi/2$, the scattering matrix elements of the AB-scatterer given by Eqs (33) and (34) are independent of Φ when L_R is even, and depend on Φ when L_R is odd. However $\langle c_p^\dagger c_{p+1} \rangle$ oscillates and varies as a function of Φ both for even and odd values of L_R , as shown in Fig. 12 and Fig. 13.

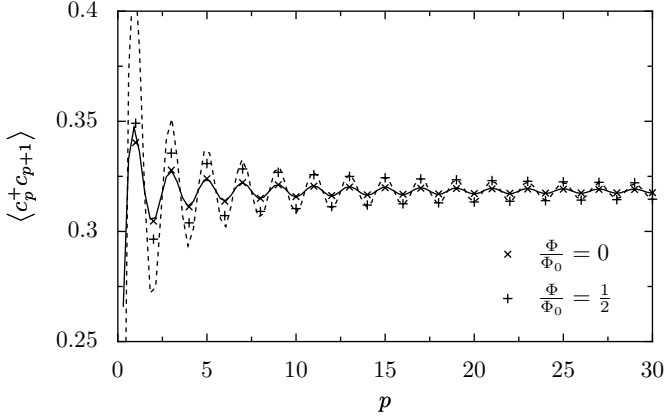


Fig. 12. Flux dependent oscillations of $\langle c_p^\dagger c_{p+1} \rangle$ towards the asymptotic value $1/\pi$, induced by an AB scatterer with a ring of size $L_R = 6$, for $\Phi = \Phi_0/2$ (+) or $\Phi = 0$ (x) ($k_F = \pi/2$ and $L'_c = 4$). The dashed and solid lines give two asymptotic fits $1/\pi + b \cos(\pi p + c)/p$ with ($b = 0.09983$, $c = \pi$) and ($b = 0.02746$, $c = \pi$) for $\Phi = \Phi_0/2$ and $\Phi = 0$ respectively.

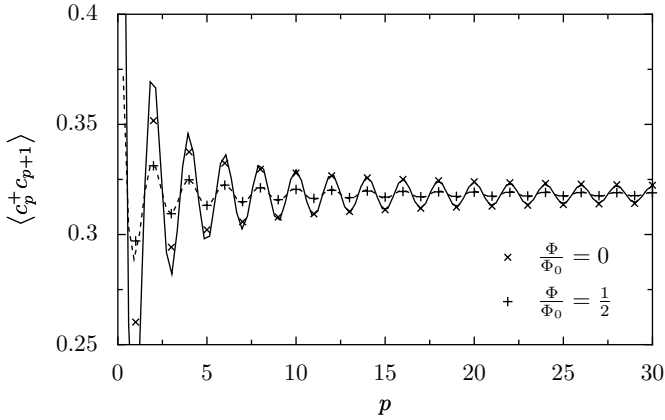


Fig. 13. Flux-dependent oscillations of $\langle c_p^\dagger c_{p+1} \rangle$ towards the asymptotic value $1/\pi$, induced by an AB scatterer with a ring of size $L_R = 7$ for $\Phi = \Phi_0/2$ (+) and $\Phi = 0$ (x) respectively, for $k_F = \pi/2$ and $L'_c = 4$. The dashed and solid lines give two asymptotic fits $1/\pi + b \cos(\pi p + c)/p$ with ($b = 0.027997$, $c = 0$) and ($b = 0.11029$, $c = 0$) for $\Phi = \Phi_0/2$ and $\Phi = 0$ respectively.

6 Role of the AB flux upon the nano-system transmission $|t_s|^2$

When the two scatterers are put in series, the oscillations of the first interfere with the oscillations of the second, and the solutions of Eqs. (35) have to be determined self-consistently. To calculate analytically as in subsection 2.1 $\langle c_0^\dagger c_1 \rangle$, $\langle c_0^\dagger c_0 \rangle$ and $\langle c_1^\dagger c_1 \rangle$ becomes complicated in the presence of the AB scatterer. It is simpler to obtain v , V_0 and V_1 using the numerical method given in subsection 2.2. Once v , V_0 and V_1 are known, the effective transmission amplitude t_s at an energy $E = -2 \cos k$ is given by

$$t_s(k) = \frac{-2ie^{2ik}t_c^2v \sin k}{F(V_0)F(V_1) - v^2}, \quad (37)$$

where $F(V) = 2 \cos k + V - e^{ik}t_c^2$.

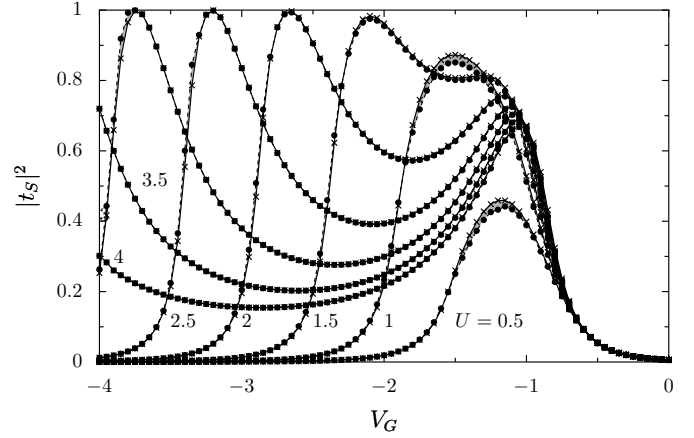


Fig. 14. Effective transmission $|t_s|^2$ as a function of the gate voltage V_G , at a filling $1/8$ (Fermi momentum $k_F = \pi/8$) and a nano-system hopping term $t_d = 0.1$. The AB-scatterer with its attached ring ($L'_c = 4$, $L_R = 7$) is at $L_c = 2$ sites from the nano-system. The interaction strength U is indicated in the figure. A flux $\Phi = 0$ (\bullet) or $\Phi = \Phi_0/2$ (x) threads the ring. The grey areas underline the effect of Φ upon $|t_s|^2$.

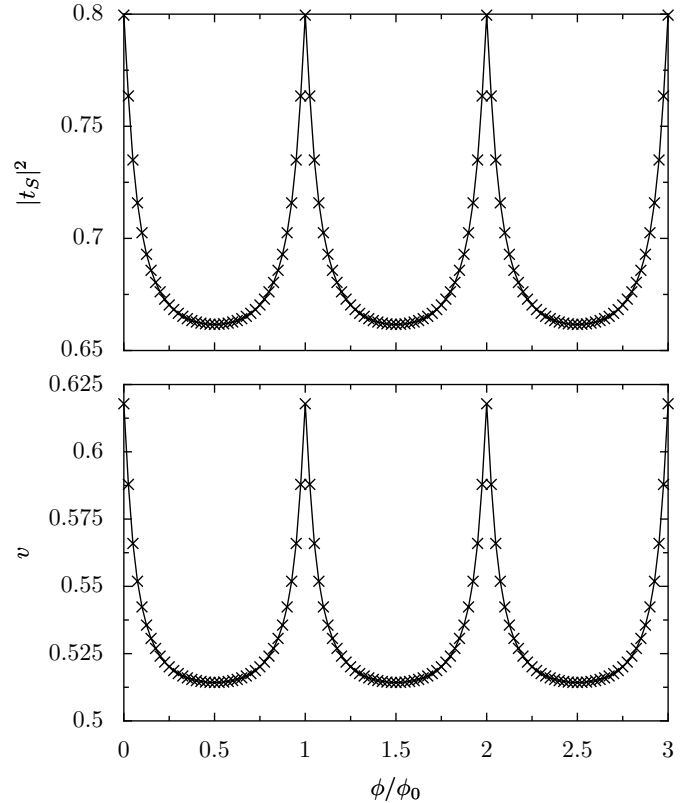


Fig. 15. Effective transmission $|t_s|^2$ (upper figure) and renormalized hopping v (lower figure) as a function of Φ/Φ_0 , for $k_F = \pi/2$, $U = 2$ and $V_G = -1$. Same values as in Fig. 2 ($L_c = 2$, $L'_c = 4$ and $L_R = 7$ and $t_d = 0.1$). Particle-hole symmetry ($k_F = \pi/2$, $V_G = -U/2$) gives $V_0 = V_1 = 0$.

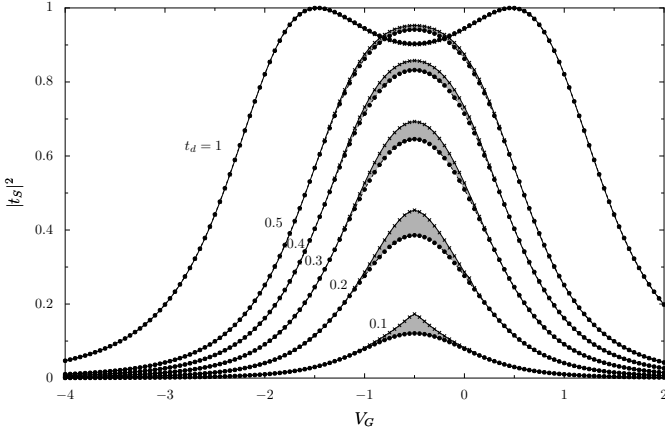


Fig. 16. Effective transmission $|t_s|^2$ as a function of V_G for different values of the nano-system hopping term t_d indicated in the figure. $k_F = \pi/2$, $L_c = 2$, $L'_c = 4$, $L_R = 7$, $U = 1$. A flux $\Phi = 0$ (\bullet) or $\Phi = \Phi_0/2$ (\times) threads the ring. The grey areas underline the effect of Φ upon $|t_s|^2$.

For having large effects of the AB flux Φ upon $|t_s|^2$, we have taken a small value $t_d = 0.1$ for the nano-system hopping term. The results are shown as a function of V_G in Fig. 14 for $k_F = \pi/8$. The ring is attached $L_c = 2$ sites away from the nano-system. The effect of Φ upon $|t_s|^2$ is indicated in Fig. 14 as in Fig. 2, by grey areas between the curves $|t_s(V_G)|^2$ obtained with $\Phi = 0$ and $\Phi = \Phi_0/2$. The effect can be seen, but remains small for $k_F = \pi/8$. The period $\lambda_F/2 = 8$ of the Friedel oscillations being larger than the nano-system size, it is likely that a stronger effect occurs if this period is reduced and becomes of the order of the nano-system size, when $\lambda_F/2 = 2$. This is confirmed in the Fig. 2 which we have put in the introduction. Those large effects are the result of the Φ -dependence of v , V_0 and V_1 . The effect being particularly large in Fig. 2 when $V_G = -1$ and $U = 2$, we show in Fig. 15 the corresponding AB oscillations characterizing $|t_s|^2$ and v when Φ varies through the ring. As shown in Fig. 2, $|t_s|^2$ takes its largest value when $V_G = -U/2$, as far as U is not too large and does not split the transmission peak. At $k_F = \pi/2$, this value of V_G yields particle-hole symmetry. Therefore, the transmission is maximum when V_G compensates the Hartree terms, such that $V_0 = V_1 = 0$ without the AB-scatterer, the only source of scattering being due to the hopping term $v \neq t_h$. One can also see in Fig. 2 that the largest dependence of $|t_s|^2$ upon Φ occurs for $V_G = -U/2$ at $k_F = \pi/2$.

The role of t_d upon the strength of the non local effect is illustrated in Fig. 16 for $k_F = \pi/2$ and $U = 1$. The dependence of Φ upon $|t_s|^2$ cannot be seen at the used scale when $t_d = 1$. This is also a value of t_d where Eq. (26) gives a good approximation of $|t_s|^2$ (see Fig. 9). When t_d decreases, the grey areas underlining the role of Φ upon $|t_s|^2$ increase around $V_G = -U/2$, where there is particle-hole symmetry. Of course, $|t_s|^2 \rightarrow 0$ as $t_d \rightarrow 0$.

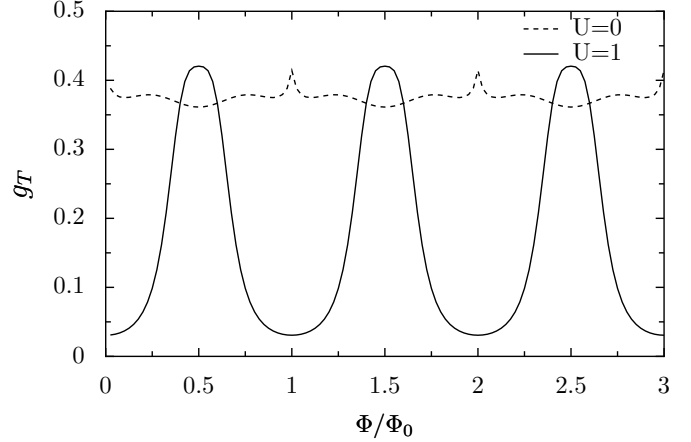


Fig. 17. Quantum conductance g_T of the nano-system and the AB-scatterer in series as a function of Φ/Φ_0 , when $U = 0$ (dotted line) and $U = 1$ (solid line). $L_c = 4$, $L_R = 7$, $L'_c = 6$, $V_G = -0.5$ and $k_F = \pi/2$. The AB-oscillations occurring without interaction ($\sin(k_F L_R) \neq 0$) are strongly increased when $U = -2V_G$.

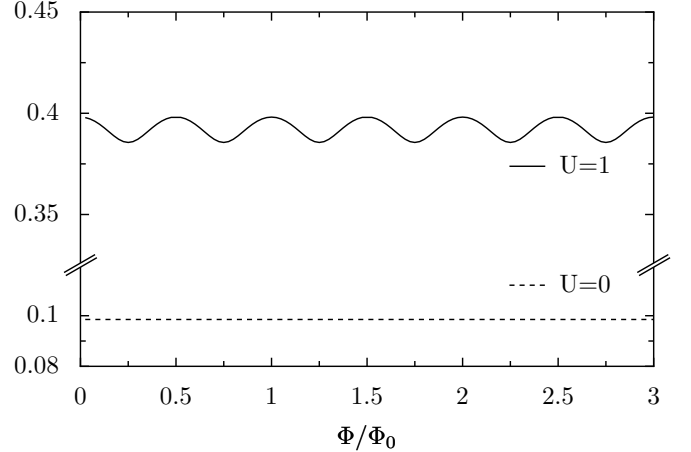


Fig. 18. g_T as a function of Φ/Φ_0 , when $U = 0$ (dotted line) and $U = 1$ (solid line). $L_c = 4$, $L_R = 6$, $L'_c = 5$, $V_G = -0.5$ and $k_F = \pi/2$. Without interaction, there are no AB-oscillations ($\sin(k_F L_R) = 0$). The interaction inside the nano-system increases g_T when $U = -2V_G$ and yields AB-oscillations.

7 Quantum conductance g_T

In the two probe geometry described by Fig. 1, the quantum conductance g_T of the nano-system and the AB-scatterer in series is given by Landauer formula which reads $g_T = |t_T(E_F)|^2$ (in units of e^2/h) in the limit where the temperature $T \rightarrow 0$. Using the HF approximation, the nano-system becomes an effective one body scatterer when $T \rightarrow 0$ and the total transmission amplitude $t_T(E_F)$ is given by the combination law valid for one body scatterers:

$$t_T(E_F) = t_s(E_F) \frac{e^{ik_F L_c}}{1 - r'_s(E_F) r_{AB}(E_F) e^{2ik_F L_c}} t_{AB}(E_F). \quad (38)$$

$r'_s(E_F)$ ($r_{AB}(E_F)$) is the reflection amplitude of the nano-system (of the AB-detector) at E_F . Because $r_{AB}(E_F)$ and $t_{AB}(E_F)$ depend in general on Φ , $g_T(E_F)$ exhibits AB-oscillations even without interaction or if L_c is very large, limits where $t_s(E_F)$ and $r'_s(E_F)$ are independent of Φ . However, when the electrons interact inside the nano-system and if L_c is not too large, $t_s(E_F)$ and $r'_s(E_F)$ exhibit also AB-oscillations which can be important around certain values of V_G and which can strongly modify the AB-oscillations of the total conductance g_T . This is shown in Fig. 17 for a case where the AB-oscillations of g_T are weak without interaction, and become important when the electrons interact inside the nano-system. However, since our model depends on many parameters, it is difficult to draw a simple conclusion. There are also values of those parameters for which the AB-oscillations are large without interaction, the interaction reducing g_T and its oscillations.

In our model, there are also special cases where $\sin(k_F L_R) = 0$, such that the ring is perfectly reflecting and the AB-scatterer becomes independent of Φ at E_F . We show such a case in Fig. 18 where $k_F = \pi/2$ and $L_R = 6$, for which the interaction increases the value of g_T (the Hartree terms compensating the value of V_G when $U = -2V_G$) and yields AB-oscillations which are a pure many body effect. This is because the AB-scatterer is independent of Φ only at E_F , but not below E_F . Therefore the HF parameters, and hence $t_s(E_F)$ and $r'_s(E_F)$, have AB-oscillations which are responsible for the AB-oscillations of g_T , while $t_{AB}(E_F)$ and $r_{AB}(E_F)$ are independent of Φ for $k_F L_R = n\pi$.

8 Conclusion

In summary, we have found an effect of electron-electron interactions upon quantum transport, using the scattering approach to transport and the Hartree-Fock approximation. The study was restricted to the 1d limit with a temperature $T \rightarrow 0$ and spin polarized electrons. We have shown that the HF description of a double site nano-system becomes trivial if $t_d > t_h$, while the electron density inside the nano-system can become very sensitive to external scatterers if $t_d < t_h$. This is also if $t_d < t_h$ that it becomes possible to strongly vary the effective nano-system transmission by external scatterers. The external scatterer which we have considered contains a ring, and can give rise to flux dependent Friedel oscillations if the flux through the ring is varied. We have shown that those long range Friedel oscillations can induce AB oscillations of the effective transmission, though the ring is attached at a distance L_c from the nano-system. As explained in Ref. [15], this non local effect vanishes if the distance between the nano-system and the external scatterer exceeds the thermal length L_T (length upon which an electron propagates at the Fermi velocity during a time \hbar/kT).

It will be of course very interesting to observe this many-body effect in a transport measurement. As it is well known, the strength of the interaction becomes more important when the electron density is reduced, the Coulomb

to kinetic energy ratio (factor r_s) becoming large. A possibility is to take for the interacting nano-system a quantum dot where the electron density can be reduced by an electrostatic gate, creating a small region of large factor r_s embedded between two larger regions of larger electron density. To have strictly 1d leads with negligible electron-electron interactions is certainly not realistic. If one uses semi-conductor heterostructures, to be outside the Luttinger-Tomonaga limit requires to take at least quasi-1d leads, if not 2d electron gases (2DEGs) of high enough densities. If the leads become two dimensional, the non local effect should have a faster decay ($1/L_c^2$, instead the $1/L_c$) with $\lambda_F/2$ oscillations. If the leads remain quasi-1d, the decay will be slower.

Eventually, let us mention transport measurements [21, 22, 23] imaging coherent electron flow from a quantum point contact (QPC) where the non local effect induced by electron-electron interaction could play a role. They are made using a 2DEG created in a GaAs/AlGaAs heterostructure. A QPC cut the 2DEG in two parts, and a charged AFM tip can be scanned around the QPC. The QPC conductance g is measured as a function of the AFM tip position. When g takes a low value, the QPC is almost closed and the electron density is low around it, making very likely non negligible interaction effects. Let us note that such effects are believed to be crucial for the observed $0.7 (2e^2/h)$ structure [24]. In the case of Refs. [21, 22, 23], the QPC is biased such that its conductance is on the first conductance plateaus ($g \approx 1, 2, 3$ in units of $2e^2/h$). In that case, the QPC provides an interacting nano-system, while the external scatterer is given by the charged tip which creates a local depletion region in the 2DEG directly below it. It is observed that g is changed when the tip is scanned around the QPC, the change $\delta g(L)$ being of order of a fraction of $2e^2/h$ and decaying [21] as $1/L^2$ with the distance L between the QPC and the tip. Moreover, a 2d plot of $g(L)$ as a function of the tip position shows [21] fringes spaced by half the Fermi wave length $\lambda_F/2$. Therefore, the position-dependent conductance has exactly the behavior which one can expect if it is related to the mechanism described in this work, i. e. the behavior of Friedel oscillations in two dimensions. We leave to a further work a study of this 2d set-up, for knowing if a quantitative description of the measured $\delta g(L)$ does not require to go beyond the non interacting electron picture, making necessary to take into account our non local effect, at least when g is on the low conductance plateaus.

9 Acknowledgments

We thank M. Sanquer for drawing our attention to Refs. [21, 22, 23] and D. Weinmann for useful comments. The support of the network ‘‘Fundamentals of nanoelectronics’’ of the EU (contract MCRTN-CT-2003-504574) is gratefully acknowledged.

References

1. R. Landauer, IBM J. Res. Dev. **1**, 223 (1957)

2. M. Büttiker, Phys. Rev. Lett. **57**, 1761 (1986)
3. Y. Imry, *Introduction to Mesoscopic Physics*, Oxford University Press (1997)
4. R.A. Molina, P. Schmitteckert, D. Weinmann, R.A. Jalabert, G.-L. Ingold, and J.-L. Pichard, Eur. Phys. J. B **39**, 107 (2004)
5. S.R. White, Phys. Rev. Lett. **69**, 2863 (1992); Phys. Rev. B **48**, 10345 (1993)
6. *Density Matrix Renormalization – A New Numerical Method in Physics*, ed. by I. Peschel, X. Wang, M. Kaulke and K. Hallberg, Lecture Notes in Physics, Vol. 528, Springer, Berlin (1999)
7. R.A. Molina, D. Weinmann, R.A. Jalabert, G.-L. Ingold, and J.-L. Pichard, Phys. Rev. B **67**, 235306 (2003)
8. R.A. Molina, D. Weinmann, and J.-L. Pichard, Europhys. Lett. **67**, 96 (2004)
9. A.O. Gogolin and N.V. Prokof'ev, Phys. Rev. B **50**, 4921 (1994)
10. J. Favand and F. Mila, Eur. Phys. J. B **2**, 293 (1998)
11. O.P. Sushkov, Phys. Rev. B **64**, 155319 (2001)
12. V. Meden and U. Schollwöck, Phys. Rev. B **67**, 193303 (2003)
13. T. Rejec and A. Ramšak, Phys. Rev. B **68**, 035342 (2003)
14. R.A. Molina, D. Weinmann, and J.-L. Pichard, Eur. Phys. J. B **48**, 243 (2005)
15. Y. Asada, A. Freyn and J.-L. Pichard, Eur. Phys. J. B **53**, 109 (2006)
16. M.A. Ruderman and C. Kittel, Phys. Rev. **96**, 99 (1954)
17. K. Yosida, Phys. Rev. **106**, 893 (1957)
18. J.H. Van Vleck, Rev. Mod. Phys. **34**, 681 (1962)
19. A. Blandin and J. Friedel, J. Phys. Rad. **20**, 160 (1956)
20. A. Freyn and J.-L. Pichard, arXiv:cond-mat/0611155, to appear in Phys. Rev. Lett. , (May 2007)
21. M.A. Topinka, B.J. LeRoy, S.E.J. Shaw, E.J. Heller, R.M. Westervelt, K.D. Maranowski and A.C. Gossard, Science **289**, 2323 (2000)
22. M.A. Topinka, B.J. LeRoy, R.M. Westervelt, S.E.J. Shaw, R. Fleischmann, E.J. Heller, K.D. Maranowski and A.C. Gossard, Letters to Nature **410**, 183 (2001)
23. B.J. LeRoy, A.C. Bleszynski, K.E. Aidala, R.M. Westervelt, A. Kalben, E.J. Heller, S.E.J. Shaw, K.D. Maranowski and A.C. Gossard, Phys. Rev. Lett. **94**, 126801 (2005)
24. K.J. Thomas, J.T. Nicholls, M.Y. Simmons, M. Pepper, D.R. Mace and D.A. Ritchie, Phys. Rev. Lett. **77**, 135 (1996)